

# Inferring the effective start dates of non-pharmaceutical interventions during COVID-19 outbreaks

Ilia Kohanovski<sup>1</sup>, Uri Obolski<sup>2,3</sup>, and Yoav Ram<sup>1,4,a</sup>

<sup>1</sup>School of Computer Science, Interdisciplinary Center Herzliya, Herzliya 4610101, Israel

<sup>2</sup>School of Public Health, Faculty of Medicine, Tel Aviv University, Tel Aviv 6997801, Israel

<sup>3</sup>Porter School of the Environment and Earth Sciences, Faculty of Exact Sciences, Tel Aviv University, Tel Aviv 6997801, Israel

<sup>4</sup>School of Zoology, Faculty of Life Sciences, Tel Aviv University, Tel Aviv 6997801, Israel

<sup>a</sup>Corresponding author: yoav@yoavram.com, ORCID 0000-0002-9653-4458

January 26, 2021

## Abstract

**Background.** During Feb-Apr 2020, many countries implemented non-pharmaceutical interventions, such as school closures and lockdowns, with variable schedules, to control the COVID-19 pandemic caused by the SARS-CoV-2 virus. Overall, these interventions seem to have reduced the spread of the pandemic. We hypothesized that the official and effective start date of such interventions can be noticeably different, for example due to slow adoption by the population, or because the authorities and the public are unprepared, and that these difference can lead to errors in the estimation of the impact of NPIs.

**Methods.** SEIR models were fitted to case data from 12 regions to infer the effective start dates of interventions and contrast them with the official dates.

**Results.** We infer mostly late, but also early effects of interventions. For example, Italy implemented a nationwide lockdown on Mar 11, but we infer the effective start date on Mar 17 ( $^{+3.05}_{-2.01}$  days 95% CI). In contrast, Germany announced a lockdown on Mar 22, but we infer an effective start date on Mar 19 ( $^{+0.92}_{-0.99}$  days 95% CI). Moreover, we find that the impact of NPIs can be under-estimated if assuming they start at their official date.

**Conclusions.** Differences between the official and effective start of NPIs are likely, and that neglecting such differences can lead to under-estimation of the impact of NPIs.

Keywords: SEIR, COVID-19, public health, epidemic, infectious disease, NPI

## 30 Introduction

32 The COVID-19 pandemic has resulted in implementation of extreme non-pharmaceutical interventions  
34 (NPIs) in many affected countries. These interventions, from social distancing to lockdowns, are  
36 applied in a rapid and widespread fashion. NPIs are designed and assessed using epidemiological  
models, which follow the dynamics of infection to forecast the effect of different mitigation and  
suppression strategies on the levels of infection, hospitalization, and fatality. These epidemiological  
models usually assume that the effect of NPIs on infection dynamics begins at the officially declared  
date<sup>9,11,17</sup>.

38 Adoption of public-health recommendations is often critical for effective response to infectious diseases, and has been studied in the context of HIV<sup>15</sup> and vaccination<sup>5,24</sup>, for example. However,  
40 behavioural and social change does not occur immediately, but rather requires time to diffuse in the population through media, social networks, and social interactions. Moreover, compliance to NPIs  
42 may differ between different interventions and between people with different backgrounds. For example, in a survey of 2,108 adults in the UK during Mar 2020, Atchison et al.<sup>2</sup> found that those over  
44 70 years old were more likely to adopt social distancing than young adults (18-34 years old), and that those with lower income were less likely to be able to work from home and to self-isolate. Similarly,  
46 compliance to NPIs may be impacted by personal experiences. Smith et al.<sup>21</sup> have surveyed 6,149 UK adults in late Apr 2020 and found that people who believe they have already had COVID-19 are  
48 more likely to think they are immune, and less likely to comply with social distancing guidelines. Compliance may also depend on risk perception as perceived by the the number of domestic cases or  
50 even by reported cases in other regions and countries. Interestingly, the perceived risk of COVID-19 infection has likely caused a reduction in the number of influenza-like illness cases in the US starting  
52 from mid-Feb 2020<sup>25</sup>.

54 Here, we hypothesize that there is a significant difference between the official start of NPIs and their effective adoption by the public and therefore their effect on infection dynamics. We use a *Susceptible-Exposed-Infected-Recovered* (SEIR) model and a *Markov Chain Monte Carlo* (MCMC) parameter

**Table 1: Official start of non-pharmaceutical interventions.**

Country	First	Last
Austria	Mar 10 2020	Mar 16 2020
Belgium	Mar 12 2020	Mar 18 2020
Denmark	Mar 12 2020	Mar 18 2020
France	Mar 13 2020	Mar 17 2020
Germany	Mar 12 2020	Mar 22 2020
Italy	Mar 5 2020	Mar 11 2020
Norway	Mar 12 2020	Mar 24 2020
Spain	Mar 9 2020	Mar 14 2020
Sweden	Mar 12 2020	Mar 18 2020
Switzerland	Mar 13 2020	Mar 20 2020
United Kingdom	Mar 16 2020	Mar 24 2020
Wuhan	Jan 23 2020	Jan 23 2020

The date of the first intervention is for a ban of public events, or encouragement of social distancing, or for school closures. In all countries except Sweden, the date of the last intervention ( $\tau^*$ ) is for a lockdown. In Sweden, where a lockdown was not ordered during the studied dates, the last date is for school closures. Dates for European countries from Flaxman et al.<sup>9</sup>, date for Wuhan, China from Pei and Shaman<sup>20</sup>. See Figure S1 for a visual presentation.

56 estimation framework to infer the effective start date of NPIs from publicly available COVID-19 case  
 58 data in 12 geographical regions. We compare these estimates to the official dates, and find that they  
 60 include both late and early effects of NPIs on infection dynamics. We conclude by demonstrating  
 how differences between the official and effective start of NPIs can confound assessments of their  
 impacts.

## Results

62 Several studies have described the effects of non-pharmaceutical interventions in different geographical  
 64 regions<sup>9,11,17</sup>. Some of these studies have assumed that the parameters of the epidemiological model  
 66 change at a specific date (Eq. 6), and set the change date  $\tau$  to the official NPI date  $\tau^*$ , usually the  
 lockdown start date (Table 1). They then fit the model once for time  $t < \tau^*$  and once for time  $t \geq \tau^*$ .  
 68 For example, Li et al.<sup>17</sup> estimate the infection dynamics in China before and after  $\tau^*$ , which is set at  
 Jan 23, 2020. Thereby, they effectively estimate the transmission and reporting rates before and after  
 $\tau^*$  separately.

Here, we estimate the joint posterior distribution of the effective start date of NPIs,  $\tau$ , and the  
 70 transmission and reporting rates before and after  $\tau$  from the entire data, rather than splitting the data  
 at  $\tau$ . This is done under the simplifying assumption that all interventions start at a specific date, despite

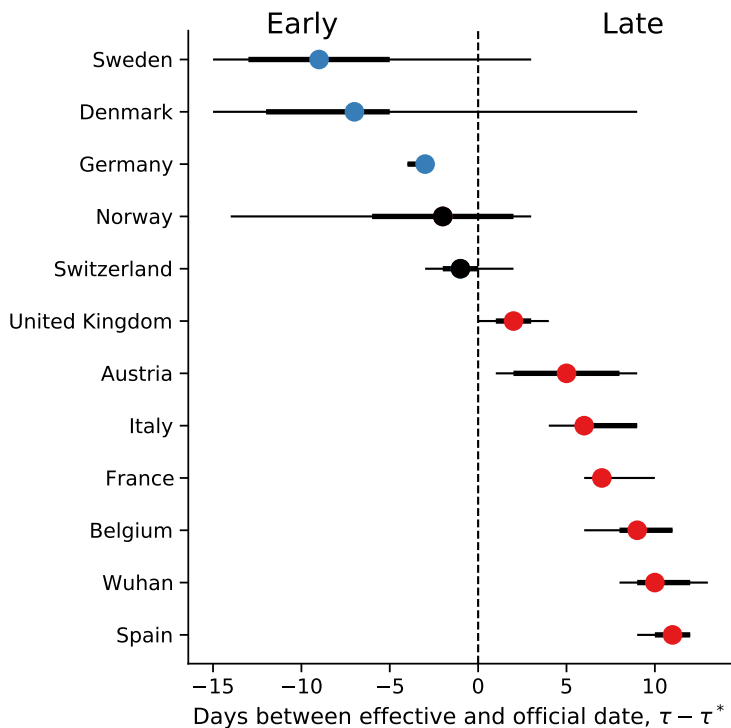


**Figure 1: Official vs. effective start of non-pharmaceutical interventions.** The difference between  $\tau$  the effective and  $\tau^*$  the official start of NPIs is shown for different regions. The effective date is delayed in UK, Austria, Italy, France, Belgium, Spain, and Wuhan, China, compared to the official date (red markers). In contrast, the estimated effective dates in Sweden, Denmark, and Germany are earlier than the official dates (blue markers), although uncertainty is low only for Germany (i.e., zero is not in 95% CI). The credible intervals for Sweden, Denmark, and Norway are especially wide, see text and Figure 3 for possible explanation. Here, the markers show  $\hat{\tau}$ , the marginal posterior median (Table 2).  $\tau^*$  is the last NPI date (a lockdown, except in Sweden; Table 1). Thin and bold lines show 95% and 75% credible intervals, respectively. Figure S2 shows a similar summary when estimating  $\hat{\tau}$  using case data up to Mar 28 rather than Apr 11.

72 the reality that the durations between the first and last NPIs were between 4 and 12 days (Table 1,  
 73 Figure S1). We then estimate  $\hat{\tau}$  as the median of the marginal posterior distribution of  $\tau$ . Credible  
 74 intervals (CI) are calculated as the highest density intervals<sup>16</sup>, and their upper and lower boundaries  
 75 are reported as  ${}^{+}_{-}$ upper in days relative to  $\hat{\tau}$ .  
 76 We compare the posterior predictive plots of a model with free  $\tau$  with those of a model with  $\tau$  fixed  
 77 at  $\tau^*$  and a model without  $\tau$  (i.e. transmission and reporting rates are constant). All three models were  
 78 fitted to case data up to Apr 11, 2020, used to predict out-of-sample case data up to Apr 24, 2020, and  
 79 these predictions were then compared to the real case data. The model with free  $\tau$  clearly produces  
 80 better and less variable predictions (Figure S3): In all 11 european countries, the expected posterior  
 81 RMSE (root mean squared error) of the out-of-sample predictions is lowest for the model with a free  $\tau$   
 82 (Table S1). When we compare the models using WAIC (Eq. 10), the model with free  $\tau$  is strongly  
 83 preferred in 9 out of 12 countries, the exceptions being Norway (only marginal preference), Sweden,  
 84 and Denmark (Table S2). Indeed, we estimate low effect of NPIs on transmission in Denmark and  
 85 Sweden (i.e.  $\lambda = 0.7$  and 0.74, respectively; see Table 2). This may interfere with the inference of  $\tau$   
 86 due to unidentifiability. Notably, the data for Sweden and Denmark do not have a single "peak" during  
 87 the evaluated dates, possibly leading to wide credible intervals on  $\tau$  (Figure 1) and poor WAIC in the  
 88 model with free  $\tau$ , whereas the duration between the first and last interventions was especially long in  
 89 Norway (Table 1).  
 90 We compare the official ( $\tau^*$ ) and effective ( $\tau$ ) start of NPIs and find that in most regions the effective  
 91 start date differs from the official date: in 10 of 12 countries the 75% credible interval on  $\tau$  does not  
 92 include  $\tau^*$  (7 of 12 countries when considering a 95% credible interval; Figure 1). The exceptions are  
 93 Norway and Switzerland (see below). The former also has a wide credible interval, perhaps because  
 94 it has the longest duration between the first and last NPIs (Table 1).

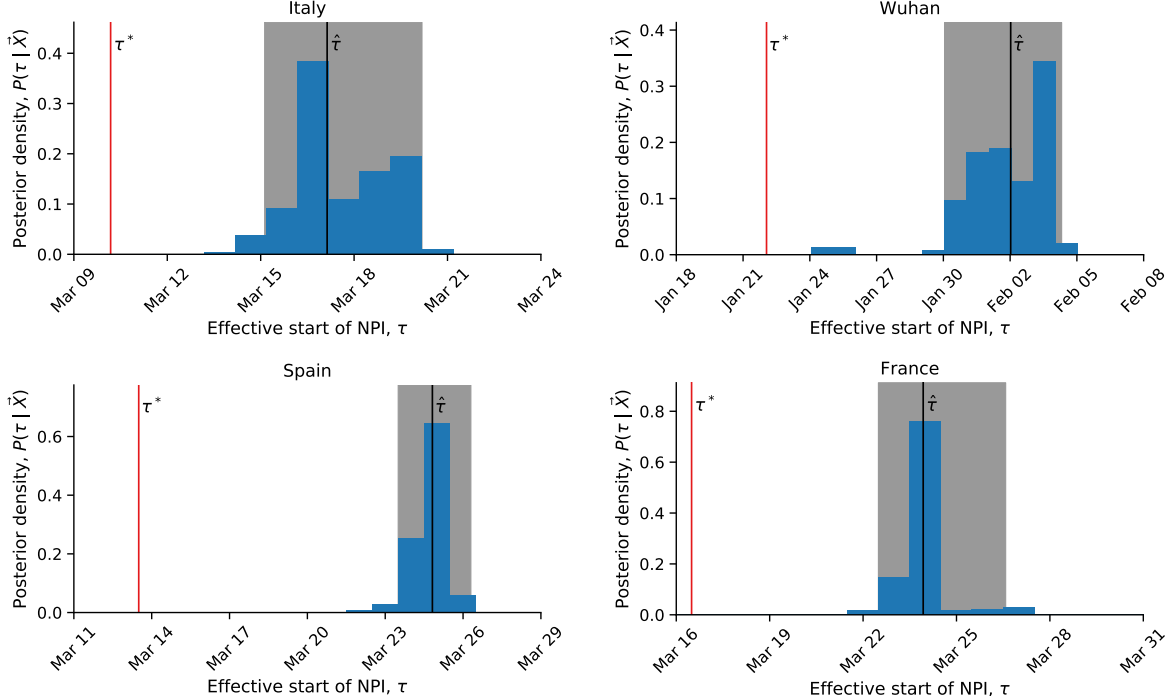


**Figure 2: Late effect of non-pharmaceutical interventions.** Posterior distribution of  $\tau$ , the effective start date of NPI, is shown as a histogram of MCMC samples. Red line shows the official last NPI date  $\tau^*$ . Black line shows the estimated effective start date  $\hat{\tau}$ . Shaded area shows a 95% credible interval.

**Late effective start of NPIs.** In half of the examined regions, we estimate that the effective start of

NPIs  $\tau$  is later than the official date  $\tau^*$ .

In Italy, the first case was officially confirmed on Feb 21. School closures were implemented on Mar 5<sup>9</sup>, a lockdown was declared in Northern Italy on Mar 8, with social distancing implemented in the rest of the country, and the lockdown was extended to the entire nation on Mar 11<sup>11</sup>. That is, the first and last official NPI dates are Mar 5 and Mar 11. However, we estimate the effective date ( $\hat{\tau}$ ) six days after the lockdown, at Mar 17 ( $^{+3.05}_{-2.01}$  days 95% CI; Figure 2).

In Wuhan, China, a lockdown was ordered on Jan 23<sup>17</sup>, but we estimate the effective start of NPIs to be ten days later, at Feb 2 ( $^{+2.29}_{-2.97}$  days 95% CI). Yet, there is low but noticeable posterior probability for Jan 25 (Figure 2), for which the effect of NPIs on transmission is considerably lower (Figure S4).

In Spain, social distancing was encouraged starting on Mar 8<sup>9</sup>, but mass gatherings still occurred on Mar 8, including a march of 120,000 people for the International Women's Day<sup>18</sup>, and a football match between Real Betis and Real Madrid (final score 2–1) with a crowd of 50,965 in Seville<sup>6</sup>. A national lockdown was only announced on Mar 14<sup>9</sup>. Nevertheless, we estimate the effective start of NPIs eleven days later, at Mar 25 ( $^{+1.70}_{-1.43}$  days 95% CI, Figure 2).

Similarly, in France we estimate the effective start of NPIs at Mar 24 ( $^{+2.65}_{-1.44}$  days 95% CI, Figure 2). This is a week later than the official lockdown, which started at Mar 17, and more than 10 days after the earliest NPI, banning of public events, which started on Mar 13<sup>9</sup>.

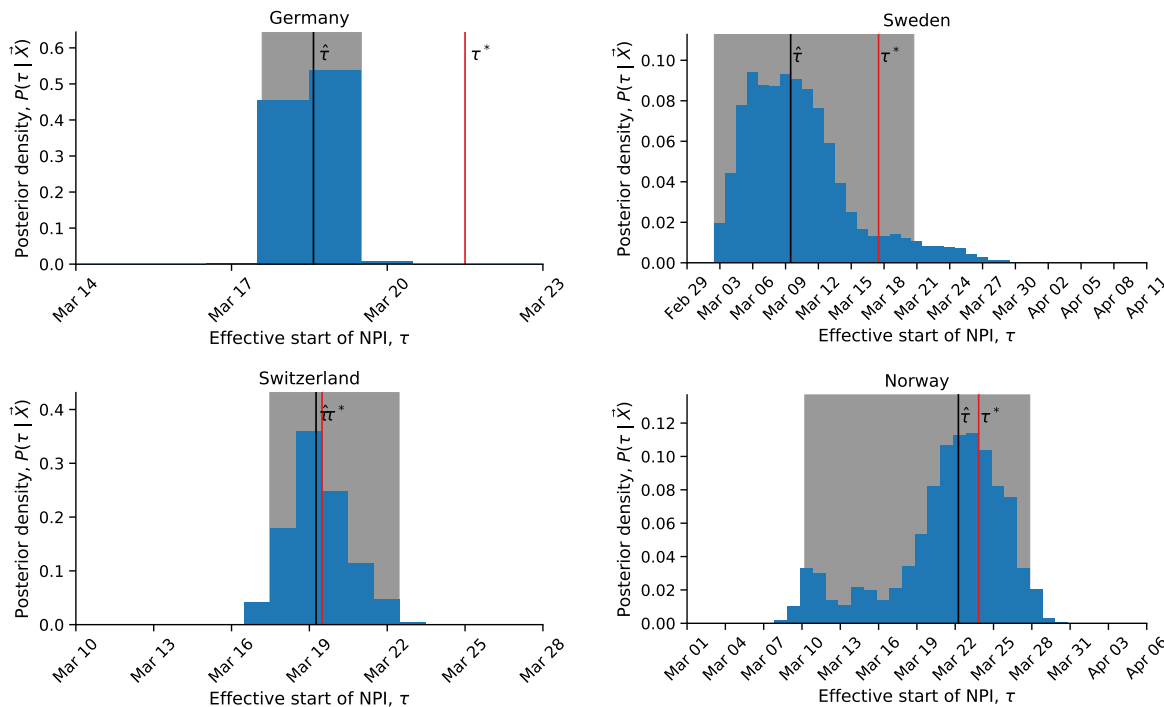


**Figure 3: Early and exact effect of non-pharmaceutical interventions.** Posterior distribution of  $\tau$ , the effective start date of NPI, is shown as a histogram of MCMC samples. Red line shows the official last NPI date  $\tau^*$ . Black line shows the estimated effective start date  $\hat{\tau}$ . Shaded area shows a 95% credible interval.

**Early effective start of NPIs.** In some regions we estimate an effective start of NPIs that is *earlier*

then the official date (Figure 1). The only conclusive early case is Germany, in which we estimate the effective start of NPIs at Mar 19 ( $^{+0.92}_{-0.99}$  days 95 %CI, Figure 3). This estimate falls between the first and last official NPI dates, Mar 12 and Mar 22 (Table 1). Therefore, when we refer to this case as "early", we mean that the effective date (Mar 19) occurs *before* the official lockdown date (Mar 22), not that

118 it occurs before all NPIs. Interestingly, Germany had the second longest duration between first and  
119 last NPIs after Norway (10 and 12 days respectively; Table 1). However, the credible interval for the  
120 effective start date in Germany is narrow (1.91 days), whereas it is very wide in Norway (17.61 days).  
121 The significantly earlier estimate of  $\hat{\tau}$  relative to  $\tau^*$  can suggest that early NPIs in Germany more  
122 effectively reduced transmission rates compared to other countries. Another possible interpretation is  
123 that the German population anticipated the lockdown and reacted before it started.

124 We also estimate an early effective start of NPIs in Denmark, Norway, and Sweden. However, the  
125 credible intervals are quite wide (Figure 1), and in Denmark and Sweden the evidence did not support  
126 the model with free  $\tau$  over the model with  $\tau$  fixed at the official date (Table S2). Indeed, Denmark  
127 and Sweden had the smallest estimated effect of NPIs on transmission rates, which probably hinders  
128 our ability to estimate  $\tau$  in these countries (Table 2). Moreover, in Sweden the number of daily cases  
129 continued to grow through Apr 11, rather than "peak" (Figure S3). In Denmark, the opposite occurred:  
130 there were seemingly two "peaks", on Mar 11 and on Apr 8 (Figure S3); the first "peak" may be a  
131 result of stochastic events, for example due to a large cluster of cases or an accumulation of tests. We  
132 suspect that these missing and additional "peaks" increase the uncertainty in our inference.

133 The estimated effective date in Norway is Mar 22, two days earlier than the official date of Mar 24.  
134 However, the posterior distribution is very wide ( $^{+5.59}_{-12.03}$  days 95% CI): it covers the range between  
135 Mar 10, two days before the first NPI, and Mar 27, three days after the last NPI (Table 1, Figure S1).  
136 The high uncertainty might be due to the long duration between the first and last NPIs; however,  
137 Germany had the second longest duration between first and last NPIs, and the corresponding posterior  
138 distribution is very narrow (Figure 3). There may also be an unidentifiability issue between  $\tau$  and the  
139 effect of NPIs on transmission (Figure S4).

140 **Exact effective start of NPIs.** We find one case in which the official and effective dates match and  
141 the credible interval is narrow. Switzerland ordered a national lockdown on Mar 20, after banning  
142 public events and closing schools on Mar 13 and 14<sup>9</sup>. Indeed, the posterior median  $\hat{\tau}$  is Mar 19  
143 ( $^{+3.2}_{-1.78}$  days 95% CI, see Figure 3). Notably, Switzerland was the first to mandate self isolation of  
144 confirmed cases<sup>9</sup>.

145 **Assessment of impact of NPIs.** The *effective reproduction number*  $R$  is the average number of  
146 secondary cases caused by an infected individual after an epidemic is already underway<sup>4</sup>. We infer  
147 model-based effective reproduction numbers before and after the implementation of NPIs from model  
148 parameters (Eq. 7). We then estimate the impact of NPIs as the relative reduction in the reproduction  
149 number<sup>9</sup>,  $\Delta R = (R_1 - R_2)/R_1$ , where  $R_1$  and  $R_2$  are the reproduction numbers before and after the  
150 start of NPIs. We compare the impacts estimated using the fixed  $\tau$  model and the free  $\tau$  model. That  
151 is, we compare the impact estimate  $\Delta R$  assuming that NPIs started at the official date  $\tau^*$ , versus the  
152 estimate when inferring the effective start of NPIs from the data.

153 Figure 4 demonstrates that estimates from the fixed  $\tau$  model (y-axis) are consistently lower than  
154 estimates from the free  $\tau$  model (x-axis), except in Sweden (SE) and Denmark (DK), in which  
155 estimation uncertainty is high. That is, assuming NPIs start at their official date leads to error in the  
156 estimation of their impact. Moreover, these errors increase with the duration of the delay between the  
157 official and effective dates (Figure S5). These results suggest that the impact of past NPIs is likely  
158 to be under-estimated by health officials and researchers if they assume NPIs start at their official  
159 dates. The estimated impact can then be interpreted as ineffectiveness of the NPIs, leading to more  
160 aggressive NPIs being applied.

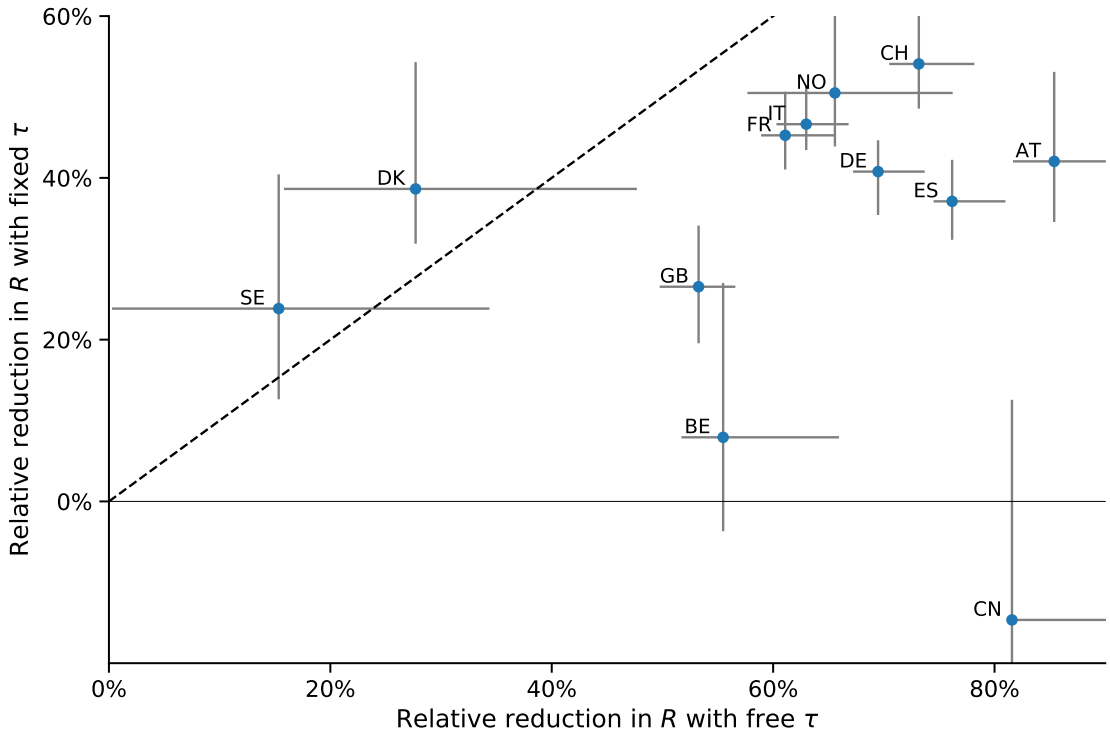


**Figure 4: Impact of NPIs is under-estimated when assuming they start at their official date.** Shown are estimates of the relative reduction in the effective reproduction number ( $R$ , see Eq. 7), which measures the impact of NPIs on the epidemic. The y-axis shows estimates when assuming the start of NPIs is fixed at the official date (fixed  $\tau$ ). The x-axis shows estimates when inferring the effective start of NPIs from the data (free  $\tau$ ). The dashed line shows a one-to-one correspondence. Markers and bars denote the posterior median and 50% credible intervals (HDI). The relative reductions in  $R$  are consistently lower for the fixed  $\tau$  model (below the dashed line), except in Sweden and Denmark in which uncertainty is high. Figure S5 shows how the delay in effective start affect the estimation error. AT: Austria, BE: Belgium, CH: Switzerland, CN: Wuhan, China, DE: Germany, DK: Denmark, ES: Spain, FR: France, GB: United Kingdom, IT: Italy, NO: Norway, SE: Sweden.

## Discussion

162 We have inferred the effective start date of NPIs in 12 regions using SEIR models under an MCMC  
 163 parameter estimation framework. We find examples of both late and early effective start of NPIs  
 164 relative to the official date (Figure 1).

In most investigated regions we find late effective start of NPIs. For example, in Italy and in Wuhan,  
 165 China, the effective start of the lockdowns seems to have occurred five or more days after the official date  
 166 (Figure 2). These differences might be explained, in some cases, by low compliance or non-adherence  
 167 to guidelines: In Italy, for example, the government plan to implement a lockdown in the Northern  
 168 provinces leaked to the public, which led to people leaving these provinces before the lockdown  
 169 started<sup>11</sup>. Late effect of NPIs may also be due to the time required by both the government and the  
 170 citizens to prepare for a lockdown, and for new guidelines to be adopted by the population.

172 In contrast, in some regions we inferred reduced transmission rates even before official lockdowns were  
 173 implemented, although this is only conclusive in Germany (Figure 3). An early effective date might be  
 174 due to early adoption of social distancing and similar behavioural adaptations in parts of the population,

possibly due to earlier NPIs or NPIs being applied in other regions. Adoption of these behaviours  
176 may occur via media and social networks, rather than official guidelines, and may be influenced by  
increased risk perception due to domestic or international COVID-19 reports<sup>1</sup>. Indeed, the evidence  
178 supports a change in infection dynamics (i.e. a model with fixed or free  $\tau$ ) even for Sweden (Table S1,  
Table S2, Figure S3), where a lockdown was not implemented within the investigated time\*.

180 Interestingly, the effective start of NPIs in France and Spain is estimated to have started on Mar 24  
and 25, respectively, although the official NPI dates differ significantly: the first NPI in France is  
182 only one day before the last NPI in Spain. The number of daily cases was similar in both countries  
until Mar 8, but diverged by Mar 13, reaching much higher numbers in Spain (Figure S6). This  
184 may suggest correlations between effective starts of NPIs in different countries due to international or  
global events.

186 As expected, we have found that the evidence supports a model in which the transmission rate changes  
at a specific time point over a model with a constant transmission rate (Tables S1 and S2). It may be  
188 interesting to check if the evidence supports a model with *two* or more change-points, rather than one.  
Multiple change-points could reflect escalating NPIs (e.g. school closures followed by lockdowns),  
190 or an intervention followed by a relaxation. However, interpretation of such models will be harder,  
as multiple change-points are also likely to result in parameter unidentifiability, for example due to  
192 simultaneous implementation of NPIs<sup>9</sup>.

As different countries experiment with various intervention strategies, we expect similar shifts to  
194 occur: in some cases the population will be late to comply with new guidelines, whereas in other cases  
the population will adopt either restrictions or relaxations even before they are formally announced.

196 Attempts to assess the impact of NPIs<sup>3,9</sup> generally assume they start at their official date. However,  
late effective start of NPIs, such as we have inferred, can lead to under-estimation of the impact of NPIs  
198 (Figures 4 and S5). Such under-estimation may lead decision-makers to enforce stricter guidelines,  
rather than enforce earlier implementation of the guidelines<sup>19</sup>.

200 Our results highlight the complex interaction between personal, regional, and global determinants of  
behavioral response to an epidemic. Therefore, we emphasize the need to further study heterogeneity  
202 in compliance and behavior over both time and space. This can be accomplished both by surveying  
differences in compliance within and between populations<sup>2</sup>, and by incorporating specific behavioral  
204 models into epidemiological models<sup>1,7,23</sup>.

## Models and Methods

206 **Data.** We use daily confirmed case data  $\mathbf{X} = (X_1, \dots, X_T)$  from 12 regions during Jan–Apr 2020. These  
incidence data summarise the number of individuals  $X_t$  tested positive for SARS-CoV-2 (using RT-qPCR tests)  
208 on each day  $t$ . Data for Wuhan, China, from Jan 10 to Feb 8, retrieved from Pei and Shaman<sup>20</sup>. Data for  
11 European countries, from Feb 20 to Apr 24, retrieved from Flaxman et al.<sup>9</sup>. Where there were multiple  
210 sequences of days with zero confirmed cases (e.g. France), we cropped the data to begin with the last sequence  
so that our analysis focuses on the first sustained outbreak rather than isolated imported cases. For official NPI  
212 dates see Table 1.

214 **SEIR model.** We model SARS-CoV-2 infection dynamics by following the number of susceptible  $S$ , exposed  
 $E$ , reported infected  $I_r$ , unreported infected  $I_u$ , and recovered  $R$  individuals in a population of size  $N$ . This  
model distinguishes between reported and unreported infected individuals: the reported infected are those that  
216 have enough symptoms to eventually be tested and thus appear in daily case reports, to which we fit the model.  
This model is inspired by Li et al.<sup>17</sup> and Pei and Shaman<sup>20</sup>, who used a similar model with multiple regions

---

\*Sweden banned public events on Mar 12, encouraged social distancing on Mar 16, and closed schools on Mar 18<sup>9</sup>.

218 and constant transmission and reporting rates to study COVID-19 dynamics in China and in the continental  
 US.  
 220 Susceptible ( $S$ ) individuals become exposed due to contact with reported or unreported infected individuals ( $I_r$   
 or  $I_u$ ) at a rate  $\beta_t$  or  $\mu\beta_t$ , respectively. The parameter  $0 < \mu < 1$  represents the decreased transmission rate  
 222 from unreported infected individuals, who are often subclinical or even asymptomatic<sup>8,22</sup>. The transmission  
 rate  $\beta_t \geq 0$  may change over time  $t$  due to behavioural changes of both susceptible and infected individuals.  
 224 Exposed individuals, after an average latent period of  $Z$  days, become reported infected with probability  $\alpha_t$  or  
 unreported infected with probability  $(1 - \alpha_t)$ . The reporting rate  $0 < \alpha_t < 1$  may also change over time due  
 226 to changes in human behaviour. Infected individuals remain infectious for an average period of  $D$  days, after  
 which they either recover, or become ill enough to be quarantined. In either case, they no longer infect other  
 228 individuals, and therefore effectively become recovered ( $R$ ). The model is described by the following set of  
 equations,

$$\begin{aligned} \frac{dS}{dt} &= -\beta_t S \left( \frac{I_r}{N} + \mu \frac{I_u}{N} \right) \\ \frac{dE}{dt} &= \beta_t S \left( \frac{I_r}{N} + \mu \frac{I_u}{N} \right) - \frac{E}{Z} \\ \frac{dI_r}{dt} &= \alpha_t \frac{E}{Z} - \frac{I_r}{D} \\ \frac{dI_u}{dt} &= (1 - \alpha_t) \frac{E}{Z} - \frac{I_u}{D} \\ \frac{dR}{dt} &= \frac{I_r}{D} + \frac{I_u}{D}, \end{aligned} \tag{1}$$

230 where  $N$  is the population size. The initial numbers of exposed  $E(0)$  and unreported infected  $I_u(0)$  are free  
 232 model parameters (i.e. inferred from the data), whereas the initial number of reported infected and recovered is  
 assumed to be zero,  $I_r(0) = R(0) = 0$ , and the number of susceptible is  $S(0) = N - E(0) - I_u(0)$ .

234 **Likelihood function.** For a given vector  $\theta$  of model parameters the *expected* cumulative number of reported  
 infected individuals ( $I_r$ ) until day  $t$ , following Eq. 1, is

$$236 \quad Y_t(\theta) = \int_0^t \alpha_s \frac{E(s)}{Z} ds, \quad Y_0 = 0. \tag{2}$$

238 We assume that reported infected individuals are confirmed and therefore observed in the daily case report of  
 day  $t$  with probability  $p_t$  (note that an individual can only be observed once, and that  $p_t$  may change over time,  
 but  $t$  is a specific date rather than the time elapsed since the individual was infected). We denote by  $X_t$  the  
 240 *observed* number of confirmed cases in day  $t$ , and by  $\tilde{X}_t$  the cumulative number of confirmed cases until end of  
 day  $t$ ,

$$242 \quad \tilde{X}_t = \sum_{i=1}^t X_i. \tag{3}$$

Therefore, at day  $t$  the number of reported infected yet-to-be confirmed individuals is  $(Y_t(\theta) - \tilde{X}_{t-1})$ . We assume  
 244 that  $X_t$  conditioned on  $\tilde{X}_{t-1}$  is Poisson distributed, such that

$$\begin{aligned} (X_1 | \theta) &\sim Poi(Y_1(\theta) \cdot p_1), \\ (X_t | \tilde{X}_{t-1}, \theta) &\sim Poi((Y_t(\theta) - \tilde{X}_{t-1}) \cdot p_t), \quad t = 2, \dots, T. \end{aligned} \tag{4}$$

246 Hence, the *likelihood function*  $\mathcal{L}(\theta | \mathbf{X})$  for a parameter vector  $\theta$  given the confirmed case data  $\mathbf{X} = (X_1, \dots, X_T)$   
 is defined by the probability to observe  $\mathbf{X}$  given  $\theta$ ,

$$248 \quad \mathcal{L}(\theta | \mathbf{X}) = P(\mathbf{X} | \theta) = P(X_1 | \theta) \cdot P(X_2 | \tilde{X}_1, \theta) \cdots P(X_T | \tilde{X}_{T-1}, \theta). \tag{5}$$

**NPI model.** To model non-pharmaceutical interventions (NPIs), we set the start of the NPIs to day  $\tau$  and define

$$\beta_t = \begin{cases} \beta, & t < \tau \\ \beta\lambda, & t \geq \tau \end{cases}, \quad \alpha_t = \begin{cases} \alpha_1, & t < \tau \\ \alpha_2, & t \geq \tau \end{cases}, \quad p_t = \begin{cases} 1/9, & t < \tau \\ 1/6, & t \geq \tau \end{cases}, \quad (6)$$

where  $0 < \lambda < 1$ . The values for  $p_t$  follow Li et al.<sup>17</sup>, who estimated the average time between infection and reporting in Wuhan, China, at 9 days before the start of NPIs and 6 days after start of NPIs.

Following Li et al.<sup>17</sup>, the effective reproduction numbers before and after the start of NPIs are

$$\begin{aligned} R_1 &= \alpha_1\beta D + (1 - \alpha_1)\mu\beta D, \\ R_2 &= \alpha_2\lambda\beta D + (1 - \alpha_2)\mu\lambda\beta D. \end{aligned} \quad (7)$$

The relative reduction in the effective reproduction number due to NPIs is  $\frac{R_1 - R_2}{R_1}$ .

**Parameter estimation.** To estimate the model parameters from the daily case data  $\mathbf{X}$ , we apply a Bayesian inference approach. Model fitting was calibrated for case data up to Mar 28, and then applied to data up to Apr 11 (for Wuhan, China, model fitting was applied for data up to Feb 8.) We start our model  $\Delta t$  days<sup>11</sup> before the outbreak (defined as consecutive days with increasing confirmed cases) in each country. The model in Eqs. 1 and 6 is parameterised by the vector  $\theta$ , where

$$\theta = (Z, D, \mu, \beta, \lambda, \alpha_1, \alpha_2, E(0), I_u(0), \Delta t, \tau). \quad (8)$$

The likelihood function is defined in Eq. 5. We defined the following prior distributions on the model parameters  $P(\theta)$ :

$$\begin{aligned} Z &\sim Uniform(2, 5) \\ D &\sim Uniform(2, 5) \\ \mu &\sim Uniform(0.2, 1) \\ \beta &\sim Uniform(0.8, 1.5) \\ \lambda &\sim Uniform(0, 1) \\ \alpha_1, \alpha_2 &\sim Uniform(0.02, 1) \\ E(0) &\sim Uniform(0, 3000) \\ I_u(0) &\sim Uniform(0, 3000) \\ \Delta t &\sim Uniform(1, 5) \\ \tau &\sim TruncatedNormal\left(\frac{\tau^* + \tau^0}{2}, \frac{\tau^* - \tau^0}{2}, 5, T - 2\right), \end{aligned} \quad (9)$$

where the prior for  $\tau$  is a truncated normal distribution shaped so that the date of the first and last NPI,  $\tau^0$  and  $\tau^*$  (Table 1), are at minus and plus one standard deviation, and taking values only between 5 and  $T - 2$ , where  $T$  is the number of days in the data  $\mathbf{X}$ . We also tested an uninformative uniform prior,  $Uniform(1, T - 2)$ . WAIC (Eq. 10) of a model with this uniform prior was either higher, or lower by less than 2, compared to WAIC of a model with the truncated normal prior. The uninformative prior resulted in non-negligible posterior probability for unreasonable  $\tau$  values, such as Mar 1 in the United Kingdom. We therefore decided to use the more informative truncated normal prior for  $\tau$ . Other priors follow Li et al.<sup>17</sup>, with the following exceptions.  $\lambda$  is used to ensure transmission rates are lower after the start of the NPIs ( $\lambda < 1$ ). We checked values of  $\Delta t$  larger than five days and found they generally produce lower likelihood and unreasonable parameter estimates, and therefore chose  $Uniform(1, 5)$  as the prior for  $\Delta t$ . We also tried to estimate the value of  $p_t$  before and after  $\tau$ , instead of keeping it fixed at 1/9 and 1/6. The model with fixed values was supported by the evidence (lower WAIC, see below) in 9 of 12 countries. Moreover, the estimates for Wuhan, China were 1/9 and 1/6, as in Li et al.<sup>17</sup>.

The posterior distribution of the model parameters  $P(\theta | \mathbf{X})$  is estimated using the affine-invariant ensemble sampler for Markov chain Monte Carlo (MCMC)<sup>13</sup>, implemented in the emcee Python package<sup>10</sup>. We use

the default configuration with the stretch move and a stretch scale parameter  $a = 2$ . For the main analysis we  
282 use 50 chains (or walkers) per region, with 7M samples per chain (no thinning was applied; 6.8M for Wuhan).  
The *integrated autocorrelation time* (IAT)<sup>10,13</sup> was averaged across parameters and chains for each region. The  
284 average IAT was between 31.9K for Wuhan and 187K for Germany (Figure S7). We examined the trace plots for  
286  $\tau$  in all regions (Figure S8). All chains seem to converge to the stationary distribution, in most cases before 2M  
288 samples. Thus, we discarded the first 2M samples as burn-in samples. The only exception is Spain, in which  
290 a single chain converged at around 6M samples. We considered this chain as part of the burn-in and removed  
292 it from the analysis. Therefore, 50 chains with 5M samples and IAT between 32K and 187K give an effective  
294 sample size between 1,336 and 7,523. We ran additional chains with 2M samples and a different initialization  
(i.e. seed). The estimated posterior distributions of  $\tau$  were very similar to our main analysis, further increasing  
our confidence in the convergence of our inference. For the models with fixed  $\tau$  and without  $\tau$ , in some countries,  
we use less than 7M samples per chain because the IAT converged sooner. In these cases the effective sample  
size was at between 2,454 (UK) and 10,954 (Spain) in the fixed  $\tau$  model and between 6,230 (Norway) and  
94,339 (Italy) in the model without  $\tau$ .

**Model comparison.** We perform model selection using two methods. First, we compute WAIC (widely  
296 applicable information criterion)<sup>12</sup>,

$$WAIC(\theta, \mathbf{X}) = -2 \log \mathbb{E}[\mathcal{L}(\theta | \mathbf{X})] + 2\mathbb{V}[\log \mathcal{L}(\theta | \mathbf{X})] \quad (10)$$

298 where  $\mathbb{E}[\cdot]$  and  $\mathbb{V}[\cdot]$  are the expectation and variance operators taken over the posterior distribution  $P(\theta | \mathbf{X})$ .  
We compare models by reporting their relative WAIC; lower is better (Table S2).  
300 We also plot posterior predictions: we sample 1,000 parameter vectors from the posterior distribution  $P(\theta | \mathbf{X})$   
fitted to data up to Apr 11, use these parameter vectors to simulate the SEIR model (Eq. 1) up to Apr 24, and plot  
302 the predicted dynamics (Figure S3). Both the accuracy (i.e. overlap of data and prediction) and the precision  
(i.e. the tightness of the predictions) are good ways to visually compare models. We also compute the expected  
304 posterior RMSE (root mean squared error) of these predictions (Table S1).

## Declarations

306 **Ethics approval and consent to participate.** Not applicable.

**Consent for publication.** Not applicable.

308 **Availability of data and materials.** We use Python 3 with NumPy, Matplotlib, SciPy, Pandas, Seaborn, and  
emcee. Source code will be publicly available under a permissive open-source license at [github.com/yoavram-lab/EffectiveNPI](https://github.com/yoavram-lab/EffectiveNPI). We used freely available data, see source code repository and above *Data* section for details.

312 **Competing interests.** The authors declare that they have no competing interests.

**Funding.** This work was supported in part by the Israel Science Foundation (3811/19 and 552/19, YR). The  
314 funding body had no role in designing, performing, or analyzing the study.

**Authors' contributions.** UO and YR designed the research. IK and YR performed the research and wrote the  
316 manuscript. All authors read and approved the final manuscript.

**Acknowledgements.** We thank Yinon M. Bar-On, Lilach Hadany, Oren Kolodny, and Zohar Yakhini.

**Table 2: Parameter estimates for different regions.**

Region	$\tau^*$	$\hat{\tau}$	$HDI_{75\%}$	$HDI_{95\%}$	Z	D	$\mu$	$\beta$	$\alpha_1$	$\lambda$	$\alpha_2$	$E(0)$	$I_u(0)$	$\Delta t$		
Austria	Mar 16	Mar 21	-2.8240	2.5130	-4.2967	3.5110	3.9362	0.6385	1.1468	0.1592	0.1370	0.2667	128.6634	111.2741	2.2407	
Belgium	Mar 18	Mar 27	-1.5528	2.3908	-3.4283	2.3908	4.0266	3.6358	0.5031	1.0780	0.2536	0.4572	0.1927	327.7634	417.8771	2.1455
Denmark	Mar 18	Mar 11	-5.3104	2.5859	-7.4123	15.7701	4.0140	3.4301	0.4149	1.0594	0.1546	0.6977	0.2041	268.2553	370.4863	2.2678
France	Mar 17	Mar 24	-0.4310	0.5557	-1.4388	2.6488	4.2107	3.0919	0.4713	1.0555	0.3823	0.3789	0.4142	412.7334	1324.2711	1.6487
Germany	Mar 22	Mar 19	-0.5544	0.9207	-0.9874	0.9205	3.3868	3.6944	0.6963	1.1670	0.1464	0.2735	0.3464	555.4142	512.6100	2.1134
Italy	Mar 11	Mar 17	-0.9537	2.4978	-2.0064	3.0463	4.1810	2.6012	0.5307	0.9845	0.5554	0.3819	0.4918	1046.1239	1934.9495	1.6776
Norway	Mar 24	Mar 22	-3.9815	4.5891	-12.0256	5.5891	4.0587	3.1077	0.3949	1.0343	0.1564	0.3105	0.2447	471.9163	828.4834	2.0465
Spain	Mar 14	Mar 25	-0.7436	0.6951	-1.4311	1.6951	4.0898	3.2785	0.5791	1.1420	0.3861	0.2521	0.3091	263.3634	866.9249	1.6239
Sweden	Mar 18	Mar 09	-4.9651	4.0108	-6.9652	11.2502	4.0167	3.3536	0.3691	1.0414	0.1304	0.7359	0.3024	398.0938	541.5147	2.4724
Switzerland	Mar 20	Mar 19	-1.5556	1.2313	-1.7802	3.1982	3.9322	3.5641	0.6174	1.1477	0.1617	0.2452	0.2787	277.1029	312.9546	2.0510
United Kingdom	Mar 24	Mar 26	-1.4515	1.2782	-2.1466	2.2780	3.9944	3.4811	0.6180	1.1208	0.1959	0.4468	0.2597	288.9485	330.3028	2.0867
Wuhan, China	Jan 23	Feb 02	-1.4380	2.0284	-2.9716	2.2892	3.7473	3.6828	0.6026	1.1391	0.1825	0.3511	0.6106800	544.0883	2.3823	

See Eq. 1 for model parameters. All estimates are posterior medians. 75% and 95% credible intervals (HDI) are given for  $\tau$  in days relative to  $\hat{\tau}$ .  $\tau^*$  is the official last NPI date (Table 1).

- [1] Arthur, R. F., Jones, J. H., Bonds, M. H. and Feldman, M. W. 2020, ‘Complex dynamics induced by delayed adaptive behavior during outbreaks’, *bioRxiv* pp. 1–23.
- [2] Atchison, C., Bowman, L. R., Vrinten, C., Redd, R., Pristerà, P., Eaton, J. and Ward, H. 2021, ‘Early perceptions and behavioural responses during the COVID-19 pandemic: a cross-sectional survey of UK adults’, *BMJ Open* **11**(1), e043577.
- [3] Banholzer, N., Weenen, E. V., Kratzwald, B. and Seeliger, A. 2020, ‘The estimated impact of non-pharmaceutical interventions on documented cases of COVID-19 : A cross-country analysis’, *medRxiv* .
- [4] Bar-On, Y. M., Flamholz, A., Phillips, R. and Milo, R. 2020, ‘SARS-CoV-2 (COVID-19) by the numbers’, *Elife* **9**.
- [5] Dunn, A. G., Leask, J., Zhou, X., Mandl, K. D. and Coiera, E. 2015, ‘Associations between exposure to and expression of negative opinions about human papillomavirus vaccines on social media: An observational study’, *J. Med. Internet Res.* **17**(6), e144.
- [6] ESPN n.d., ‘Real Madrid lose grip on La Liga lead after shock loss at Real Betis’.  
**URL:** <https://www.espn.com/soccer/match?gameId=550350>
- [7] Fenichel, E. P., Castillo-Chavez, C., Ceddia, M. G., Chowell, G., Gonzalez Parrae, P. A., Hickling, G. J., Holloway, G., Horan, R., Morin, B., Perrings, C., Springborn, M., Velazquez, L. and Villalobos, C. 2011, ‘Adaptive human behavior in epidemiological models’, *Proc. Natl. Acad. Sci. U. S. A.* **108**(15), 6306–6311.
- [8] Ferretti, L., Wymant, C., Kendall, M., Zhao, L., Nurtay, A., Abeler-Dörner, L., Parker, M., Bonsall, D. and Fraser, C. 2020, ‘Quantifying SARS-CoV-2 transmission suggests epidemic control with digital contact tracing’, *Science (80-. ).* **368**(6491), eabb6936.
- [9] Flaxman, S., Mishra, S., Gandy, A., Unwin, H. J. T., Mellan, T. A., Coupland, H., Whittaker, C., Zhu, H., Berah, T., Eaton, J. W., Monod, M., Ghani, A. C., Donnelly, C. A., Riley, S. M., Vollmer, M. A. C., Ferguson, N. M., Okell, L. C. and Bhatt, S. 2020, ‘Estimating the effects of non-pharmaceutical interventions on COVID-19 in Europe’, *Nature* (March), 1–35.
- [10] Foreman-Mackey, D., Hogg, D. W., Lang, D. and Goodman, J. 2013, ‘emcee : The MCMC Hammer’, *Publ. Astron. Soc. Pacific* **125**(925), 306–312.
- [11] Gatto, M., Bertuzzo, E., Mari, L., Miccoli, S., Carraro, L., Casagrandi, R. and Rinaldo, A. 2020, ‘Spread and dynamics of the COVID-19 epidemic in Italy: Effects of emergency containment measures’, *Proc. Natl. Acad. Sci. U. S. A.* p. 202004978.
- [12] Gelman, A., Carlin, J. B., Stern, H. S., Dunson, D. B., Vehtari, A. and Rubin, D. B. 2013, *Bayesian Data Analysis, Third Edition*, Chapman & Hall/CRC Texts in Statistical Science, Taylor & Francis.
- [13] Goodman, J. and Weare, J. 2010, ‘Ensemble Samplers With Affine Invariance’, *Commun. Appl. Math. Comput. Sci.* **5**(1), 65–80.
- [14] Kass, R. E. and Raftery, A. E. 1995, ‘Bayes Factors’, *J. Am. Stat. Assoc.* **90**(430), 773.
- [15] Kaufman, M. R., Cornish, F., Zimmerman, R. S. and Johnson, B. T. 2014, ‘Health behavior change models for HIV prevention and AIDS care: Practical recommendations for a multi-level approach’, *J. Acquir. Immune Defic. Syndr.* **66**(SUPPL.3), 250–258.

- [16] Kruschke, J. K. 2014, *Doing Bayesian Data Analysis A Tutorial with R, JAGS, and Stan*, Academic Press.
- [17] Li, R., Pei, S., Chen, B., Song, Y., Zhang, T., Yang, W. and Shaman, J. 2020, ‘Substantial undocumented infection facilitates the rapid dissemination of novel coronavirus (SARS-CoV2)’, *Science* (80-). p. eabb3221.
- [18] Minder, R. and New York Times n.d., ‘Spain Becomes Latest Epicenter of Coronavirus After a Faltering Response’.  
**URL:** <https://www.nytimes.com/2020/03/13/world/europe/spain-coronavirus-emergency.html>
- [19] Pei, S., Kandula, S. and Shaman, J. 2020, ‘Differential effects of intervention timing on COVID-19 spread in the United States’, *Science Advances* **6**(49), eabd6370.
- [20] Pei, S. and Shaman, J. 2020, ‘Initial Simulation of SARS-CoV2 Spread and Intervention Effects in the Continental US’, *medRxiv* p. 2020.03.21.20040303.
- [21] Smith, L. E., Mottershaw, A. L., Egan, M., Waller, J., Marteau, T. M. and Rubin, G. J. 2020, ‘The impact of believing you have had COVID-19 on self-reported behaviour: Cross-sectional survey’, *PLoS One* **15**(11), e0240399.
- [22] Thompson, R. N., Lovell-Read, F. A. and Obolski, U. 2020, ‘Time from Symptom Onset to Hospitalisation of Coronavirus Disease 2019 (COVID-19) Cases: Implications for the Proportion of Transmissions from Infectors with Few Symptoms’, *J. Clin. Med.* **9**(5), 1297.
- [23] Walters, C. E. and Kendal, J. R. 2013, ‘An SIS model for cultural trait transmission with conformity bias’, *Theor. Popul. Biol.* **90**, 56–63.
- [24] Wiyeh, A. B., Cooper, S., Nnaji, C. A. and Wiysonge, C. S. 2018, ‘Vaccine hesitancy ’outbreaks’: using epidemiological modeling of the spread of ideas to understand the effects of vaccine related events on vaccine hesitancy’, *Expert Rev. Vaccines* **17**(12), 1063–1070.
- [25] Zipfel, C. M. and Bansal, S. 2020, ‘Assessing the interactions between COVID-19 and influenza in the United States’, *medRxiv* (February), 1–13.

# Supplementary Material

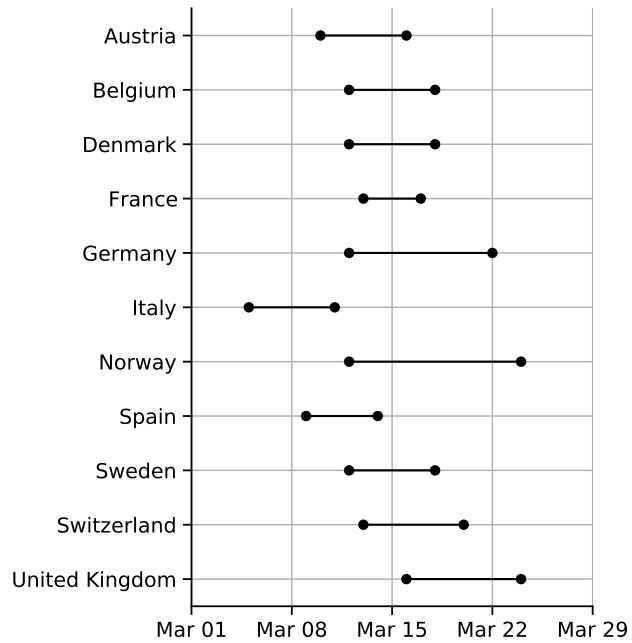


**Figure S1: Official start of non-pharmaceutical interventions.** See Table 1 for more details. Wuhan, China is not shown.

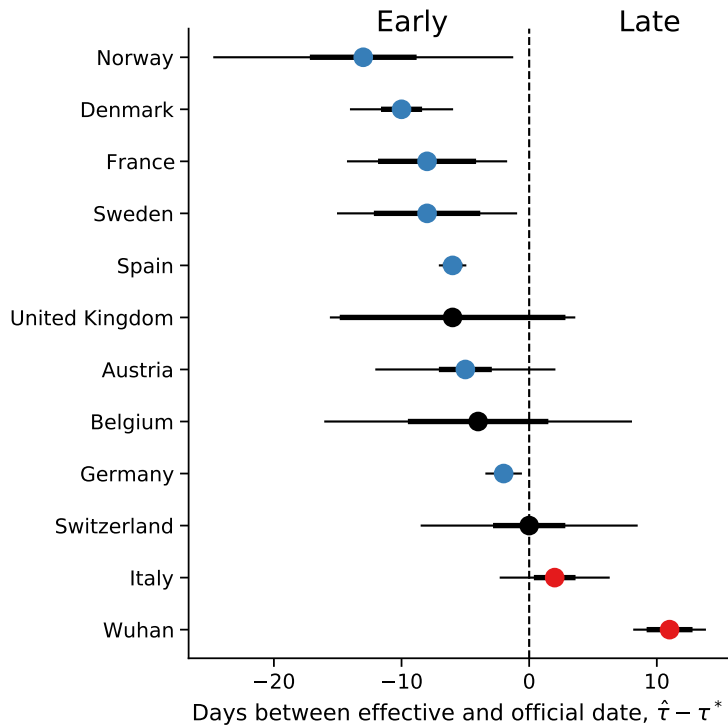


**Figure S2: Official vs. effective start of non-pharmaceutical interventions estimated up to Mar 28.** The difference between  $\tau$  the effective and  $\tau^*$  the official start of NPIs estimated from case data up to Mar 28, 2020, shown for different regions. Here,  $\hat{\tau}$  is the marginal posterior median.  $\tau^*$  is the last NPI date (a lockdown everywhere by Sweden, see Table 1). Thin and bold lines show 95% and 75% credible intervals (HDI<sup>16</sup>), respectively. Inference performed similarly to main inference, but with data up to Mar 28 and only 1M samples per chain with 600K burn-in.

**Table S1: Posterior RMSE of out-of-sample predictions with the different models.**

Country	No	Fixed	Free
Belgium	3284	2523	<b>809.5</b>
Denmark	436.5	996.8	<b>394.1</b>
France	10420	8215	<b>1714.0</b>
Germany	14620	17800	<b>1937.0</b>
Italy	15010	8827	<b>601.1</b>
Norway	295	647.1	<b>64.7</b>
Sweden	765	1206	<b>596.9</b>
Switzerland	1860	1756	<b>218.2</b>
United Kingdom	14700	14830	<b>2271.0</b>
Spain	17890	14410	<b>1180.0</b>
Austria	932.9	695.6	<b>60.6</b>

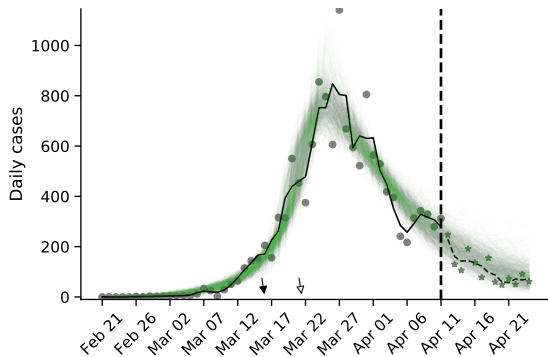
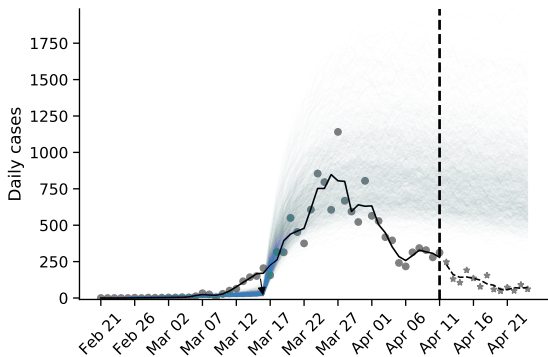
Expected posterior predictive RMSE (root mean squared error) for models with: no  $\tau$  at all, *No*;  $\tau$  fixed at the official last NPI date  $\tau^*$ , *Fixed*; and free parameter  $\tau$ , *Free*. In all cases, the model with free parameter  $\tau$  has the lowest RMSE. Models were fitted to case data up to Apr 11, 2020, and then used to generate 1,000 predictions up to Apr 24 by sampling model parameters from the posterior distribution. These predictions were then compared to the real data using RMSE, and the mean RMSE value is shown in the table for each country and model. Bold values emphasize cases in which the *Free* model has the lowest RMSE.

**Table S2: WAIC values for the different models.**

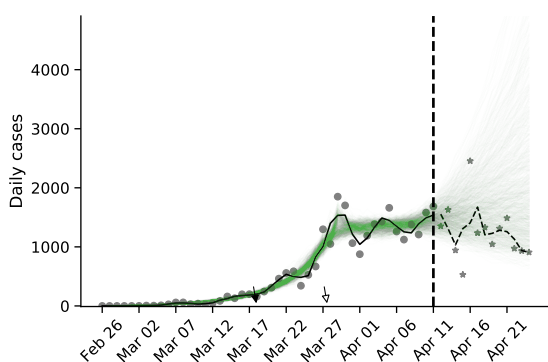
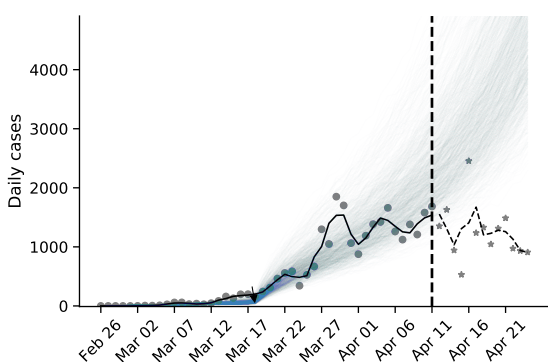
Country	No	Fixed	Free
Austria	219.45	95.56	<b>35.82</b>
Belgium	148.44	98.31	<b>45.90</b>
Denmark	44.36	<b>40.34</b>	44.93
France	581.57	255.36	<b>172.57</b>
Germany	1029.41	327.37	<b>174.97</b>
Italy	897422.87	440.16	<b>79.94</b>
Norway	69.98	41.94	<b>39.93</b>
Spain	1476.45	647.00	<b>127.92</b>
Sweden	32.59	<b>30.83</b>	30.92
Switzerland	265.95	84.39	<b>63.98</b>
United Kingdom	258.16	117.81	<b>67.41</b>
Wuhan China	107.31	94.08	<b>73.04</b>

WAIC (widely applicable information criterion; Eq. 10)<sup>12</sup> values for models with: no  $\tau$  at all, *No*;  $\tau$  fixed at the official last NPI date  $\tau^*$ , *Fixed*; and free parameter  $\tau$ , *Free*. WAIC values are scaled as a deviance measure: lower values imply higher predictive accuracy and a difference of 2 is a popular threshold for model comparison<sup>14</sup>. Bold values emphasize cases in which the *Free* model has the lowest WAIC.

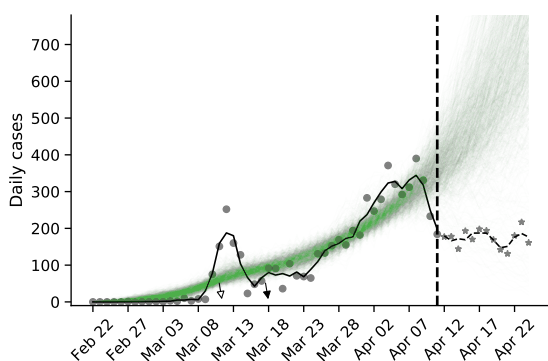
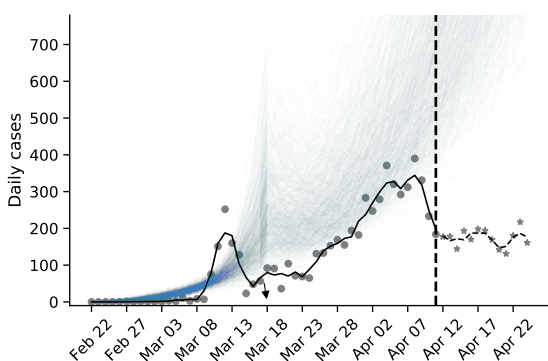
### Austria



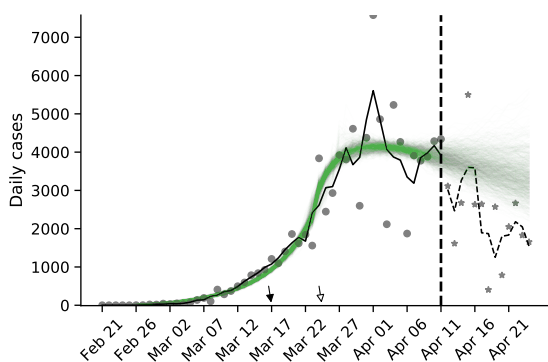
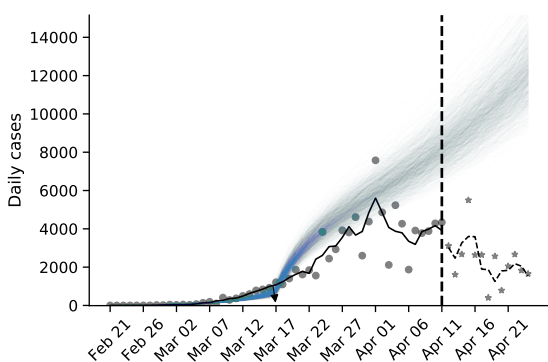
### Belgium



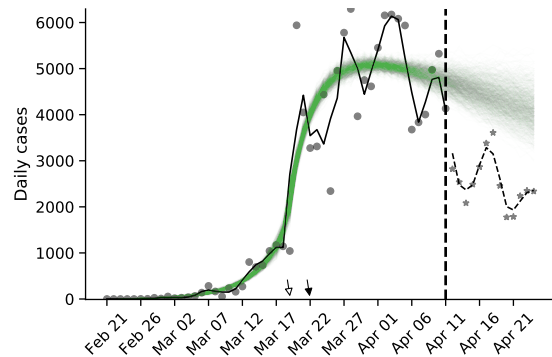
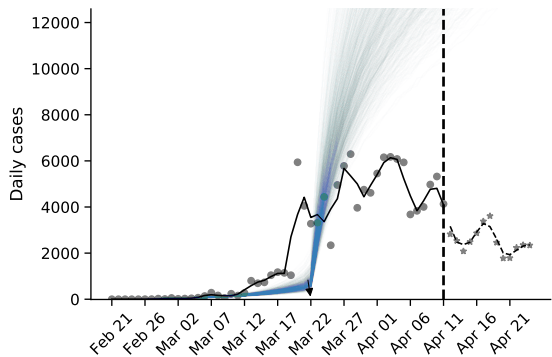
### Denmark



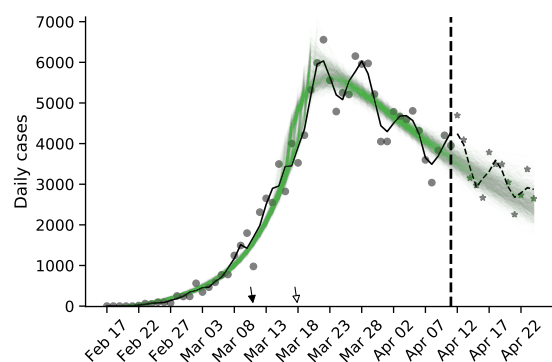
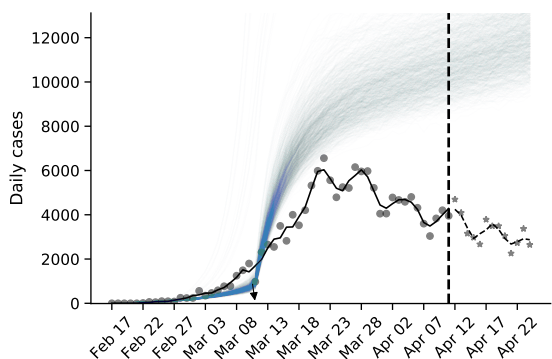
### France



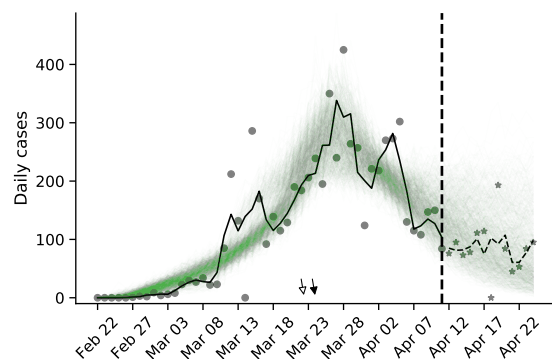
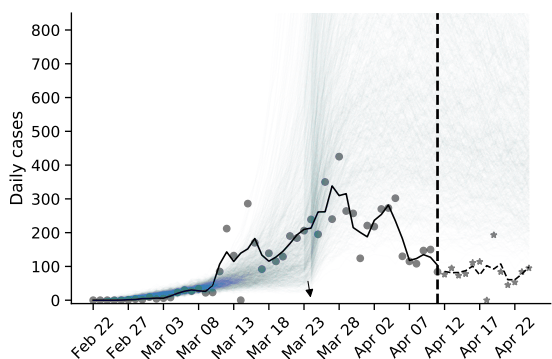
## Germany



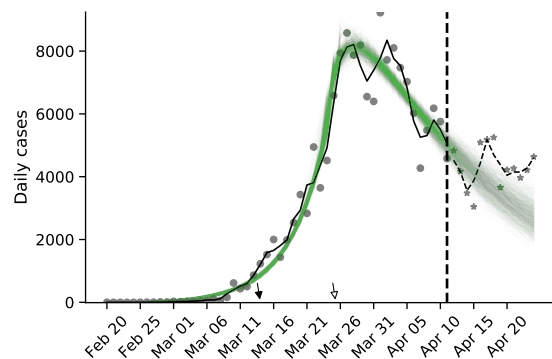
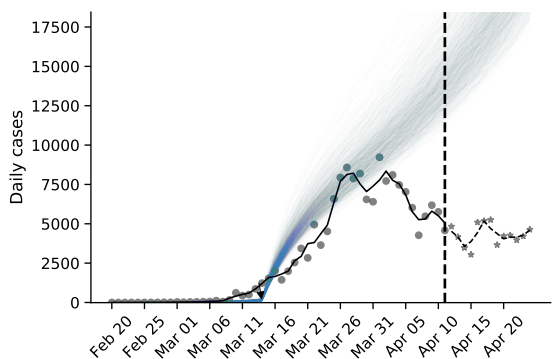
## Italy



## Norway



## Spain



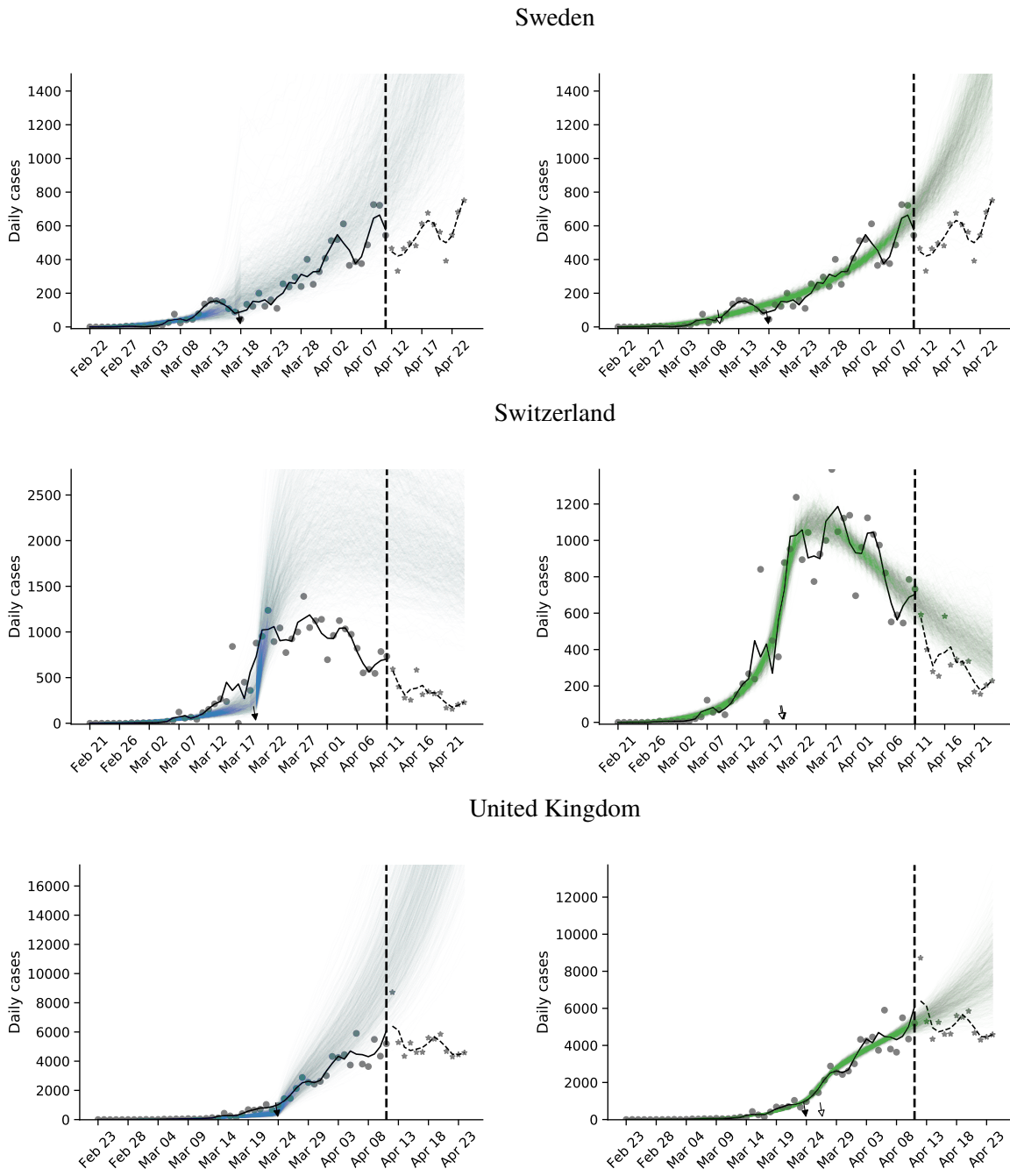


**Figure S3: Posterior prediction plots for 11 European countries.** The vertical dashed line represents Apr 11, 2020. Circles and stars represent daily case data up to and after Apr 11, respectively. Black and white arrows denote the official ( $\tau^*$ ) and effective ( $\hat{\tau}$ ) start of NPIs, respectively. Black lines represent a smoothing of the data points using a Savitzky-Golay filter with window length 3. Coloured lines represent posterior predictions from a model with fixed  $\tau$  (blue) and free  $\tau$  (green). Models were fitted with data up to Apr 11. The predictions are generated by drawing 1,000 parameter sets from the posterior distribution, and then generating a daily case count using the SEIR model (Eq. 1) up to Apr 24. Note the differences in the y-axis scale. Posterior predictions with the free  $\tau$  model predict the out-of-sample data well for all countries except Denmark and Sweden, but poorly with the fixed  $\tau$  model. The predictions of the model without  $\tau$  (not shown) are even worse.

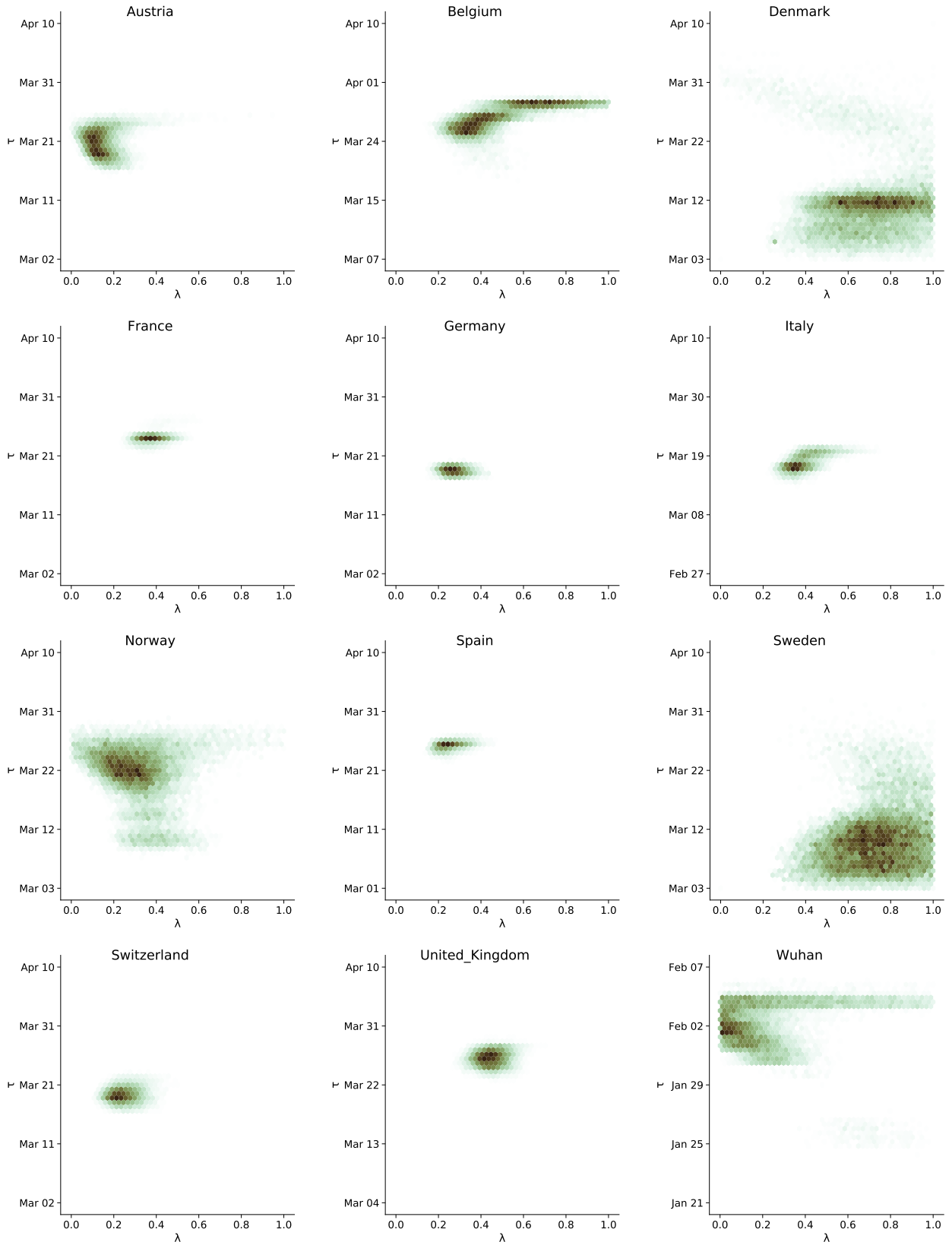


**Figure S4: Joint posterior density plots for  $\tau$  and  $\lambda$ .** The high values of  $\lambda$  estimated in Denmark and Sweden reduce the effect of the NPIs thereby making the inference of  $\tau$  more difficult, resulting in wide posterior distributions. A correlation between the parameters is also evident in Norway. In Belgium and in Wuhan a later  $\tau$  gives a wide estimate for  $\lambda$ . In comparison, Austria, France, Germany, Italy, Spain, Switzerland, and UK have a narrow joint distribution.

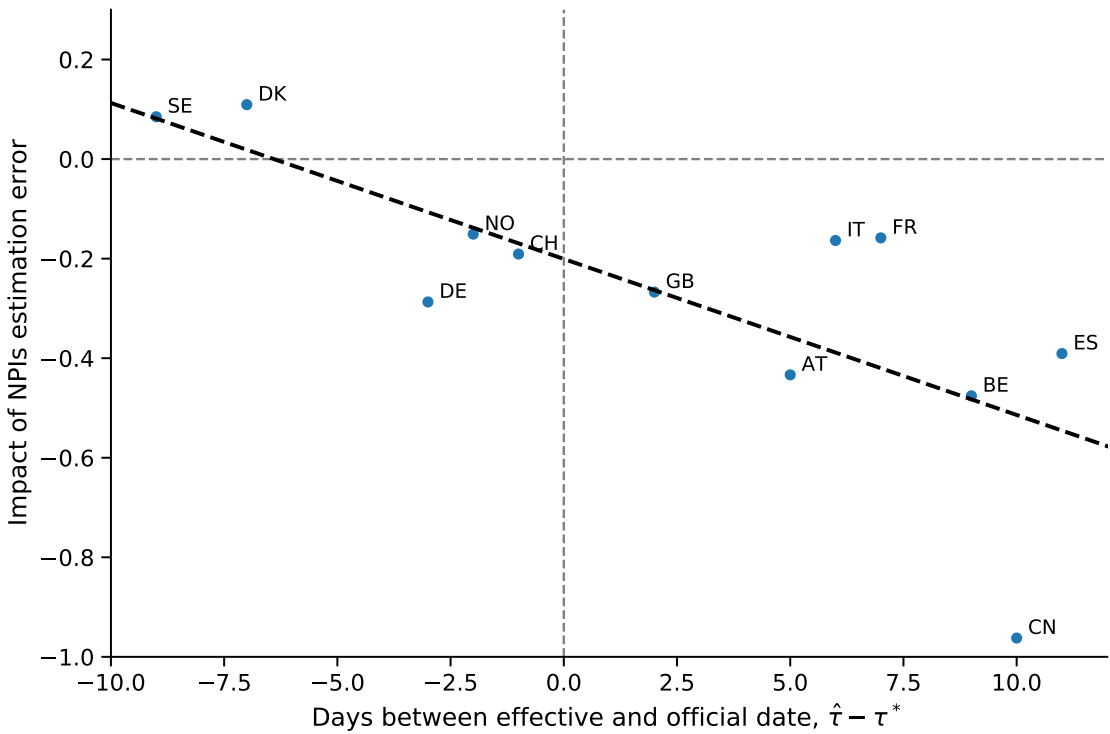


**Figure S5: Under-estimation of impact of NPIs increases with the delay in their effective start.** The x-axis shows the days between the estimated effective start of NPIs,  $\hat{\tau}$ , and the official date,  $\tau^*$ . The y-axis shows the error in estimation of the impact of NPIs when assuming they start at their official date, i.e. the difference between the median estimate from a model with fixed  $\tau$  minus the estimate from a model with free  $\tau$ , the y-axis and x-axis of Figure 4, respectively. Impact of NPIs defined as  $\frac{R_1 - R_2}{R_1}$ , where  $R_1$  and  $R_2$  are the effective reproduction numbers before and after the NPI, respectively (Eq. 7). The dashed black line shows a linear regression, slope=-0.0313 with (-0.051, -0.012) 95% CI,  $R^2 = 0.554$ . AT: Austria, BE: Belgium, CH: Switzerland, CN: Wuhan, China, DE: Germany, DK: Denmark, ES: Spain, FR: France, GB: United Kingdom, IT: Italy, NO: Norway, SE: Sweden.

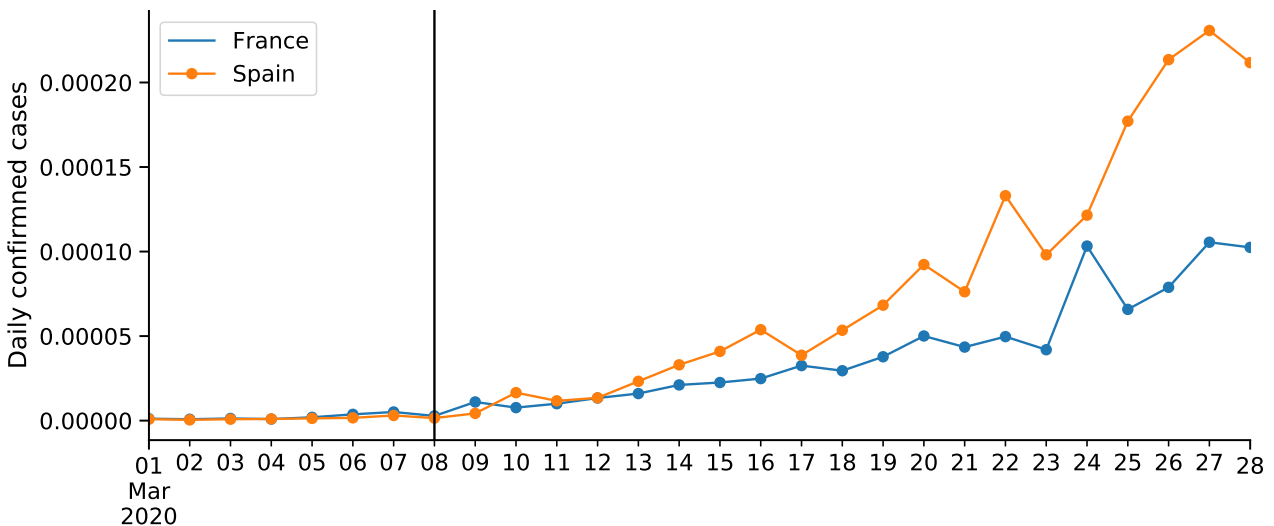


**Figure S6: COVID-19 daily confirmed cases in France and Spain.** Number of cases proportional to population size (as of 2018). Vertical line shows Mar 8, the effective start of NPIs  $\hat{\tau}$  in both countries. Data from Flaxman et al.<sup>9</sup>.

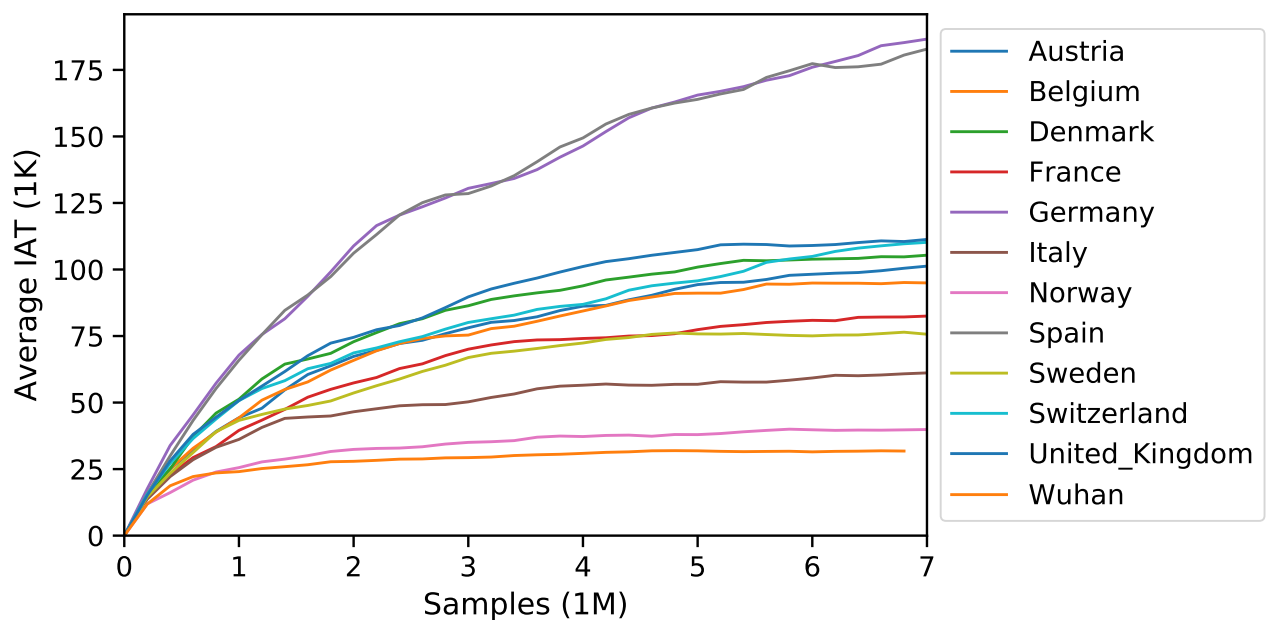


**Figure S7: Integrated autocorrelation time (IAT)<sup>10,13</sup>, averaged across model parameters and MCMC chains, as a function of the number of samples in the chains. IAT is less than 187K in all cases, while chain length is 5M after burn-in period of 2M. With 50 chains per region, this gives at least 1,335 uncorrelated samples for estimating the posterior distribution.**

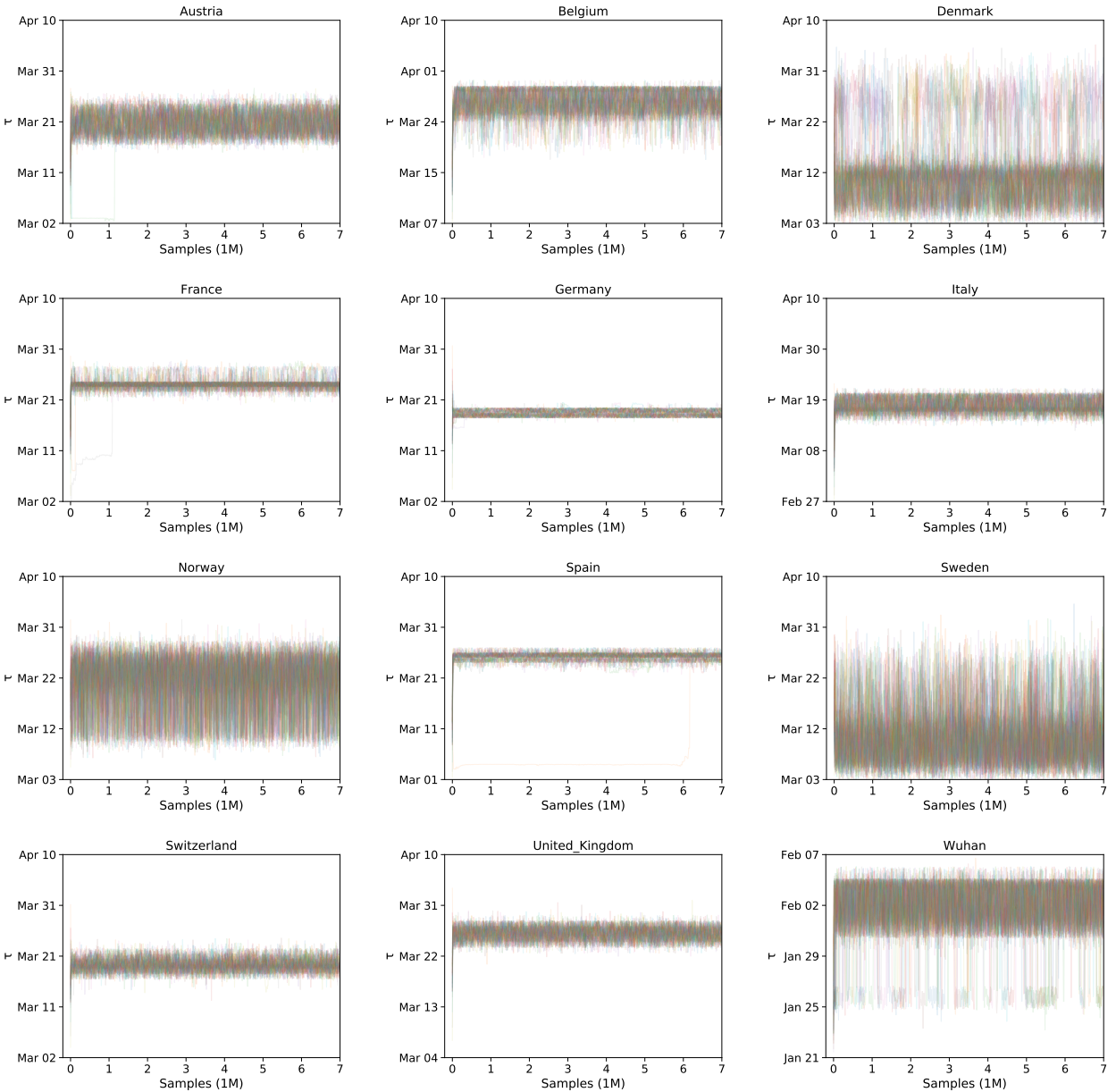


**Figure S8: Trace plots for  $\tau$ .** The value of  $\tau$  at for sequential samples of 50 chains per region. To facilitate visualization, chains were thinned 1:10,000 for the trace plots, but not for posterior estimation. Line transparency was set at  $\alpha = 0.1$  and chains cycle through different colors. In France and Austria some chains converged relatively late but before the burn-in period (2M iterations). In Spain, a single chain converged very late (after roughly 6M iterations) and was removed from further analysis. The y-axis range is the support of the prior on  $\tau$ .